2015 International Nuclear Atlantic Conference - INAC 2015
São Paulo, SP, Brazil, October 4-9, 2015
ASSOCIAÇÃO BRASILEIRA DE ENERGIA NUCLEAR - ABEN
ISBN: **978-85-99141-06-9**

FABRICATION AND CHARACTERIZATION OF SURFACE BARRIER DETECTOR FROM COMMERCIAL SILICON SUBSTRATE

Fabio Eduardo da Costa[1] and Júlio Batista Rodrigues da Silva

[1] Instituto de Pesquisas Energéticas e Nucleares (IPEN / CNEN - SP)
Av. Professor Lineu Prestes 2242
05508-000 São Paulo, SP
fecosta@ipen.br

ABSTRACT

This work used 5 silicon substrates, n-type with resistivity between 500-20,000 Ω.cm, with 12 mm diameter and 1 mm thickness, from Wacker - Chemitronic, Germany. To produce the surface barrier detectors, the substrates were first cleaned, then, they were etched with HNO_3 solution. After this, a deposition of suitable materials on the crystal was made, to produce the desired population inversion of the crystal characteristics. The substrates received a 10 mm diameter gold contact in one of the surfaces and a 5 mm diameter aluminum in the other. The curves I x V and the energy spectra for 28 keV and 59 keV, for each of the produced detectors, were measured. From the 5 substrates, 4 of them resulted in detectors and one did not present even diode characteristics. The results showed that the procedures used are suitable to produce detectors with this type of silicon substrates.

1. INTRODUCTION

A surface barrier detector is a diode semiconductor with a big area, composed of an n-type silicon crystal, with one thin side p-type doped. The reverse, also, presents characteristics of the detector, which is an n-type layer on a p-type substrate [1,2,3]. The silicon region formed between the interfaces constitutes the active region of the detector and due to a number of factors, including the purity of the silicon, it determines the maximum thickness of the active volume detector [4].

The silicon characteristics, such as atomic number of 14 and a forbidden bandwidth of 1.115 eV at 300K [5] permit that surface barrier detectors made from these crystals be capable to operate at room temperature, have small dimensions, but be restricted to the energy range detected. In this case, these energies should not be so low that they do not cross the surface barrier, the thickness of deposited gold, or so high that they are not totally absorbed within the crystal active region [5].

According to Amptek [6], for silicon detectors with thicknesses in the range from 200 to 500 µm, commercially available values, these detectors are sensitive to photons with energies between 400 eV and 100 keV, with a Gaussian distributed efficiency in this range. The sensitivity to this energy range meets the fabrication process of iodine seeds used in brachytherapy, at the Technology Center of Radiation of IPEN / CNEN-SP. These seeds, with iodine 125, send gamma rays at energies between 28 keV and 35 keV, which are suitable for detection with silicon detectors, making their development useful for the seeds laboratory preparation.

2. MATERIALS AND METHODS

In Figure 1, the five silicon substrates, as supplied by the manufacturer, can be seen.

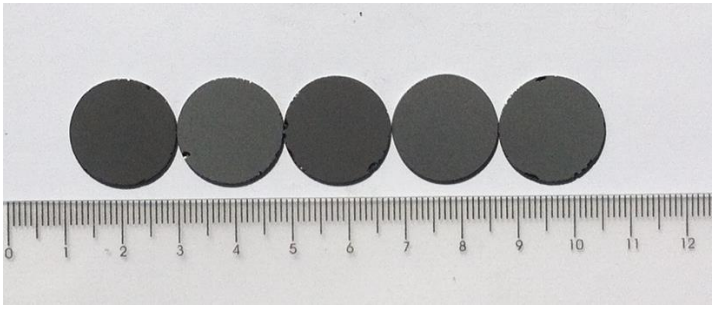

Figure 1: Commercial silicon substrates used for the fabrication of the detectors.

The 5 detectors were made following the methodology described by Shiraishi et al [7, 8]. For the initial cleaning process, a trichloroethylene solution was prepared in a polyethylene beaker, where the substrates were dipped in this solution and left under the action of an ultrasonic agitator, to remove possible residues of grease.

Subsequently, the substrates were removed from the trichloroethylene solution and introduced into another solution containing ketone. This step was finished by washing the substrates with deionized water and storage in nitric acid [1.38 N]. Further, the passivating mixture was prepared in a polyethylene beaker containing nitric acid and hydrofluoric acid, at a ratio 3: 1, with a total volume of 100 ml. In the sequence, the substrates were quickly inserted into the passivating solution with the aid of a nylon sieve and maintained in solution without letting them float. The passivation process, according to the literature, occurs at a rate of 20-30 μm/min, implying approximate time of 4 minutes for the passivation to occur in the sample completely [7, 8]. The process was interrupted with the addition of deionized water in the solution: about 2 liters were enough for the process to be finished. Only as information, the passivation process is very important to reduce noise due to the movement of charge carriers at the surface of the semiconductor detectors.

After this process, the samples were removed and again rinsed in deionized water, dried with filter paper, without being pressed to prevent any damage to the crystalline structure. Following, the substrates were bonded with epoxy resin to the fiberglass plate, only in three points, on the back of the detector. In front, they were bonded all around the boundary between the detector and the fiberglass. Then, the metals were deposited, with the help of the film evaporator, aluminum in the back and gold in the front. In Figure 2, schematic views of a detector may be seen.

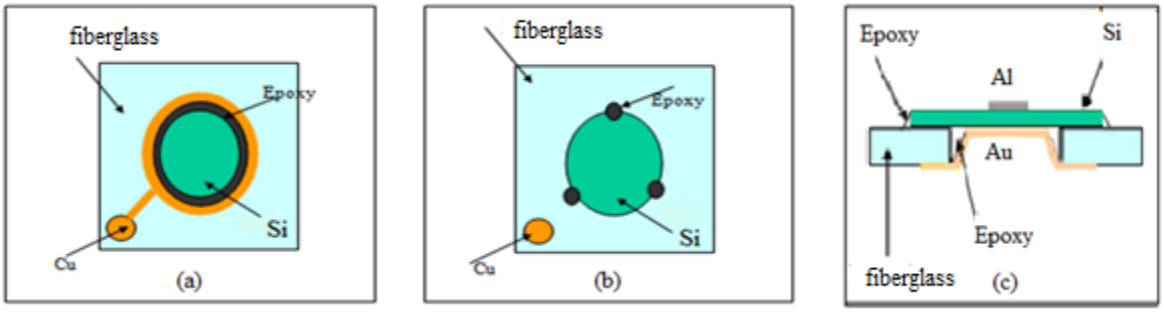

Figure 2: Schematic views of a detector: (a) is a front view of the detector; in (b), the rear part, both without receiving the metal deposition. In (c), side view of the detector shown with the deposition of metals.

The detector rear part received the aluminum deposition with only 5 mm in diameter. This reduced diameter defines the detector active volume, which is enough for determining the location of the brachytherapy seeds and, at the same time, providing the lowest capacitance of the detector to minimize the noise due to the charge sensitive pre-amplifier used in electronic system.

Further, where the aluminum film was deposited, a copper wire was glued with colloidal silver ink, to provide electrical contact. After the detectors had been finished, they were evaluated as diodes by their current x voltage curves, to ensure that rectifying junction characteristics were obtained. The rectifier feature appears in a pn junction, through the junction current behavior that has resistive characteristics in the direct polarization and nonlinear in the reverse. Two different resistor values, in the bias circuit, were used, to avoid being a limiting bias value, consequently to a possible high reverse current in the detector. These curves determined the detectors voltage operation and, in these conditions, the energy spectra were obtained.

3. RESULTS AND DISCUSSION

In Figure 3, the detectors finalized are shown: the detectors front, on the left, and their back sides, on the right.

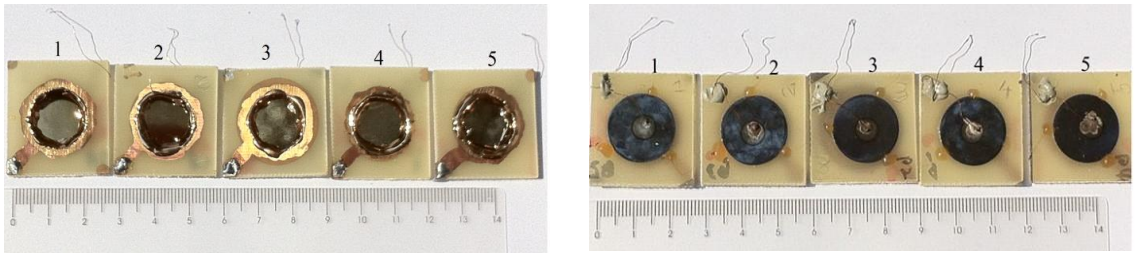

Figure 3: On the left, the front view of the detectors, where the gold deposition region can be seen; on the right, it can be seen the central region of aluminum deposition and the wires attached with colloidal silver ink to provide electrical contact with these surfaces.

3.1 Validation of detectors, such as diodes.

Figures 4 to 6 show the current x voltage curves, for each of the detectors, using 10 MΩ and 250 MΩ bias resistors.

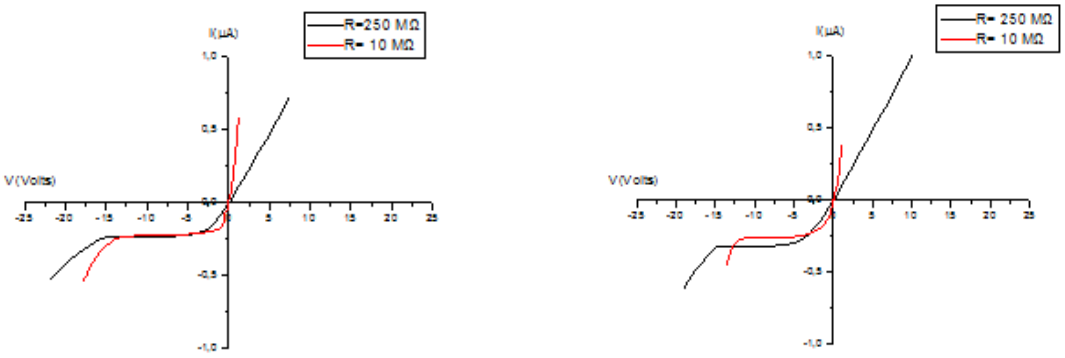

Figure 4: Current x voltage behavior: on the left for detector 1 and on the right, for detector 2.

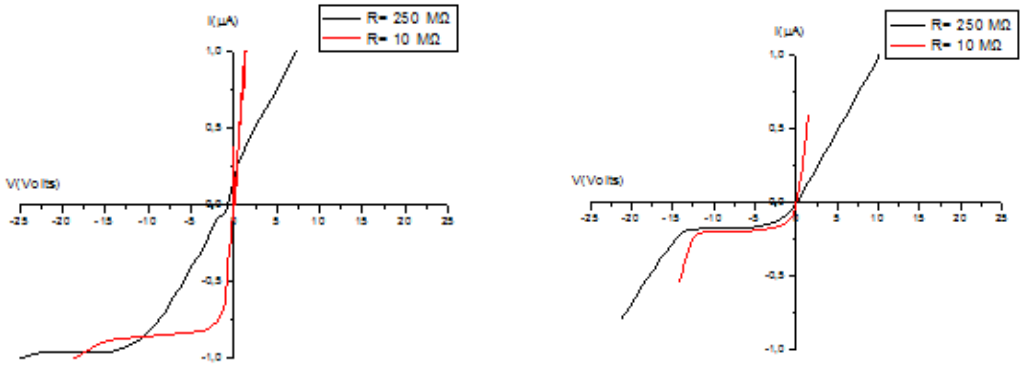

Figure 5: Current x voltage behavior: on the left for detector 3 and on the right, for detector 4.

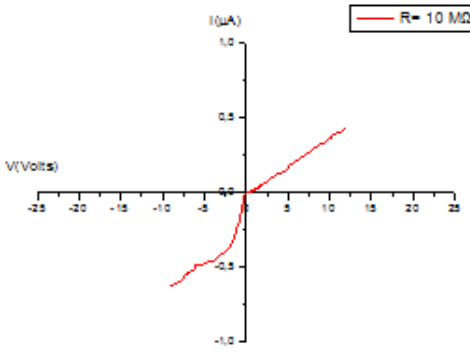

Figure 6: Current x voltage for detector 5. It was not possible to measure with the 250 MΩ bias resistor.

As it can be seen in Figures 4 to 6, the detectors 1 to 4 showed the junction behavior, with the plateau at reverse voltage, which is the region of interest for use as detectors. Detector 5 did not show this feature and did not allow the measurement with 250 MΩ bias resistors.

At Table 1, it can be seen the operating reverse voltage selected for each detector, as well as the reverse current, final thicknesses and their apparent resistivity and resistance. It can be observed that, for the resistivity of substrates (500-20000 ohm.cm), with the technique of producing a junction and operating it in reverse bias, the resistivity increases. This apparent detector resistivity minimizes the reverse detector current and, consequently, the electronic noise produced by the motion of charge carriers generated thermally. The results, from detector 5, were not included in Table 1 because it did not show plateau region and only allowed obtaining the current x voltage curve with the 10 MΩ bias resistor. It also did not allowed any measurement with a 250 MΩ bias resistor due to a greater resistance in the forward and reverse bias polarization, as it can be seen in Table 2.

Table 1: Operating reverse voltages, currents reverse, final thicknesses, resistance and apparent resistivity for each detector, with bias resistors of 10 MΩ and 250 MΩ.

Detector	$V_{reverse}$	$I_{reverse}$	Thickness	$R_{Apparent}$	$\rho_{Apparent}$
	Volts	μA	μm	MΩ	GΩ.cm
1 $R_{bias = 10\ M\Omega}$	12.6	0.22	199.0	57.3	2.2
2 $R_{bias = 10\ M\Omega}$	9.2	0.25	264.0	36.9	1.5
3 $R_{bias = 10\ M\Omega}$	11.7	0.80	135.0	14.6	1.1
4 $R_{bias = 10\ M\Omega}$	11.2	0.20	358.0	56.2	1.6
1 $R_{bias = 250M\Omega}$	14.4	0.22	199.0	65.5	2.5
2 $R_{bias = 250M\Omega}$	13.5	0.35	264.0	38.6	1.5
3 $R_{bias = 250M\Omega}$	22.5	0.95	135.0	23.6	1.8
4 $R_{bias = 250M\Omega}$	11.7	0.15	358.0	78.0	2.3

From Table 2, it can be seen that the behavior of the detector resistance, at direct polarization is similar for each bias resistor. Detector 5 (table 2, below) presented a much higher value than other detectors. This high value can be justified by an inadequate metal deposition that did not cross sufficiently through the oxide layer, produced by the surface passivation substrate.

Table 2: Direct polarization resistance values of the detectors developed.

Detector	Direct polarization resistance (MΩ)
1($R_{bias = 10\ M\Omega}$)	2.09
2($R_{bias = 10\ M\Omega}$)	2.59
3($R_{bias = 10\ M\Omega}$)	1.27
4($R_{bias = 10\ M\Omega}$)	2.61
5($R_{bias = 10\ M\Omega}$)	27.21
1($R_{bias = 250\ M\Omega}$)	10.40
2($R_{bias = 250\ M\Omega}$)	10.12
3($R_{bias = 250\ M\Omega}$)	8.24
4($R_{bias = 250\ M\Omega}$)	10.06

According to Millman and Halkias [9], a diode provides static resistance which varies with the voltage and current of the junction and, moreover, it presents a dynamic or incremental resistance that is not constant, depending on the operating point of the diode. All these contributions may justify the high resistance values in the direct polarization for the detectors developed in this work.

Figures 7 to 14 show in (a) energy gamma spectra from iodine-125, americium-241 and background noise (BG) obtained for the detectors 1 to 4, with bias resistors of 10 MΩ and 250 MΩ, and (b) with counts values standardized for better observation of differences of resolution for the two energies of gamma radiation detected. As it can be seen, all detectors showed lower efficiency at 59 keV, when compared with 28 keV energy, but this was already expected due to the reduced thickness of all detectors produced. Detector 5 did not present energy spectrum.

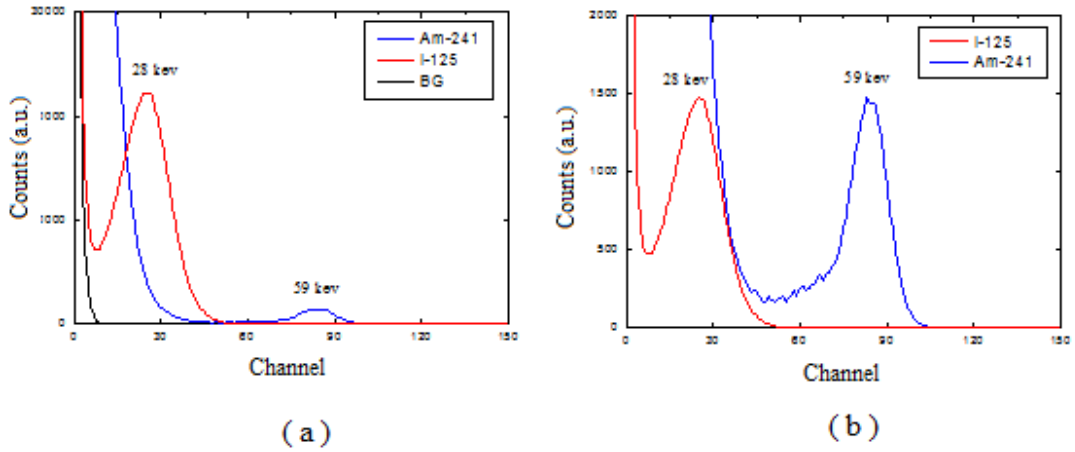

Figure 7: In (a) energy spectra of detector 1, when exposed to gamma radiation sources of iodine-125 and americium-241. In (b), the normalized spectra in counts. The spectra were measured with 10 MΩ bias resistance.

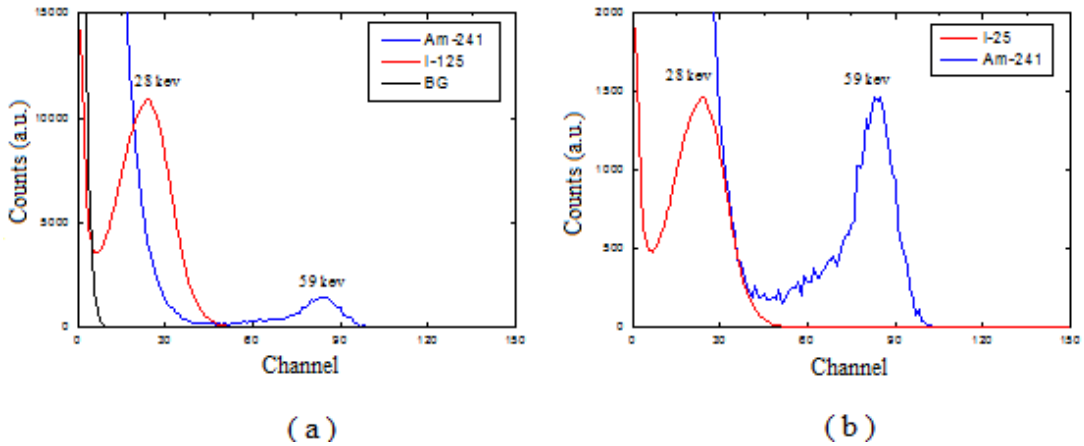

(a) (b)

Figure 8: In (a), energy spectra of detector 1, when exposed to gamma radiation sources of iodine-125 and americium-241. In (b), the normalized spectra in counts. The spectra were measured with 250 MΩ bias resistance.

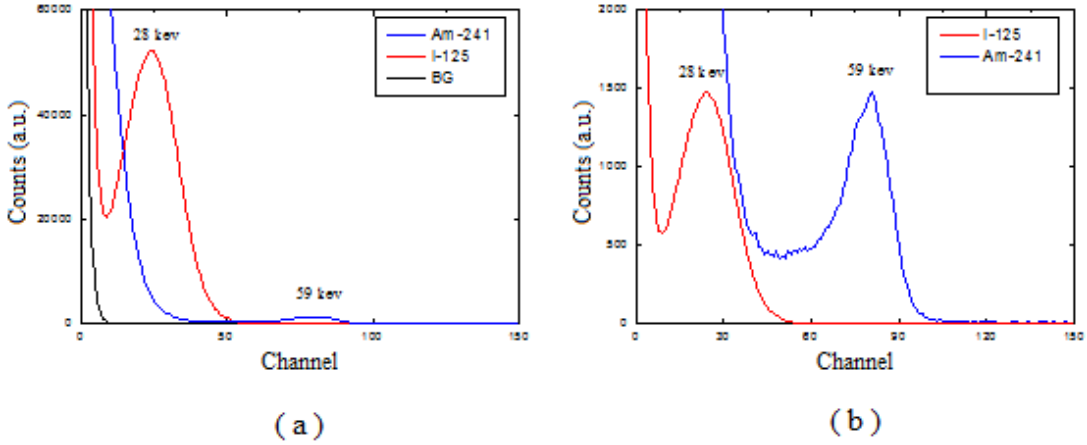

(a) (b)

Figure 9: In (a), energy spectra of detector 2, when exposed to gamma radiation sources of iodine-125 and americium-241. In (b), the normalized spectra in counts. The spectra were measured with 10 MΩ bias resistance.

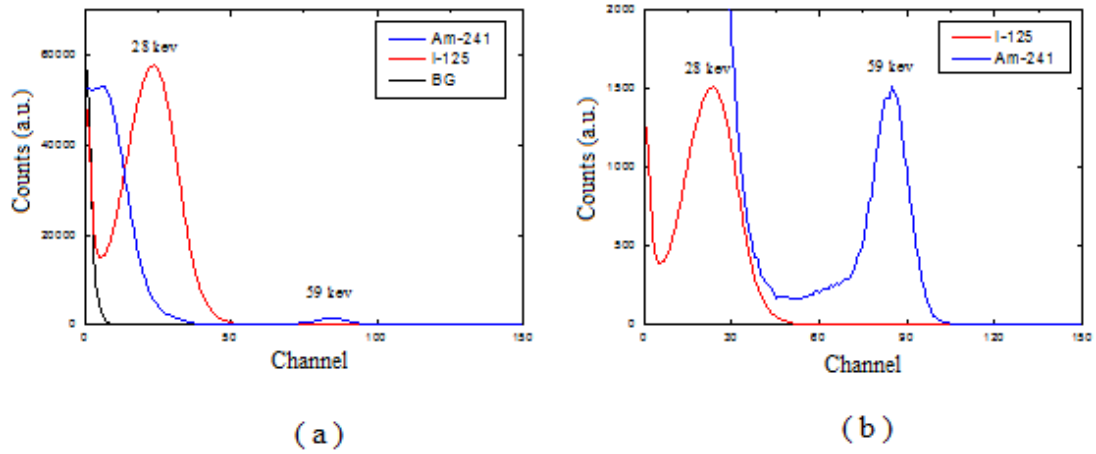

(a) (b)

Figure 10: In (a), energy spectra of detector 2, when exposed to gamma radiation sources of iodine-125 and americium-241. In (b), the normalized spectra in counts. The spectra were measured with 250 MΩ bias resistance.

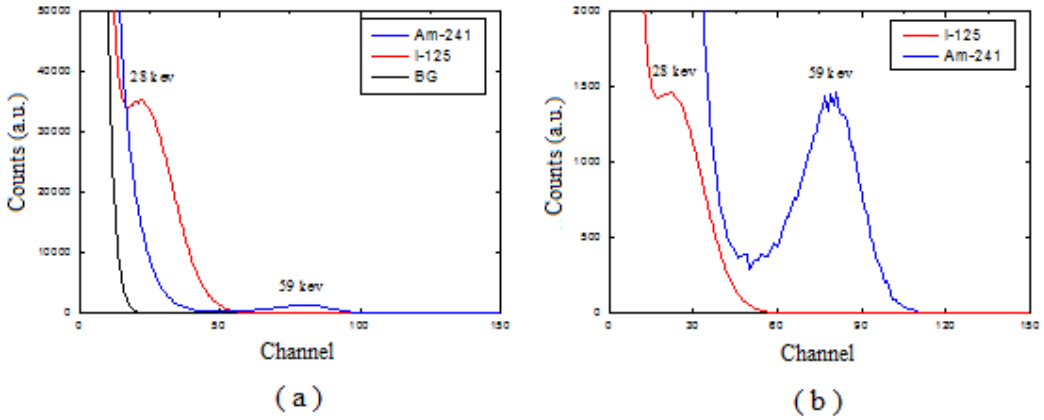

Figure 11: In (a), energy spectra of detector 3, when exposed to gamma radiation sources of iodine-125 and americium-241. In (b), the normalized spectra in counts. The spectra were measured with 10 MΩ bias resistance.

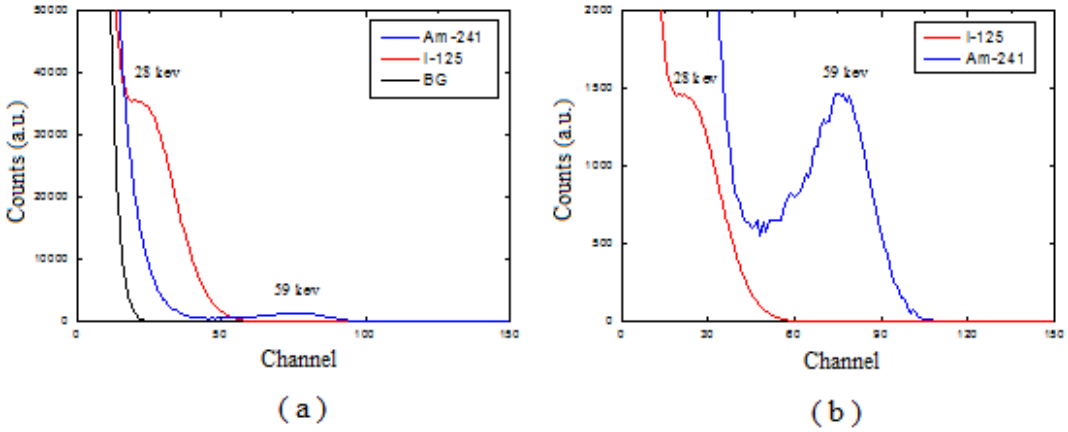

Figure 12: In (a), energy spectra of detector 3, when exposed to gamma radiation sources of iodine-125 and americium-241. In (b), the normalized spectra in counts. The spectra were measured with 250 MΩ bias resistance.

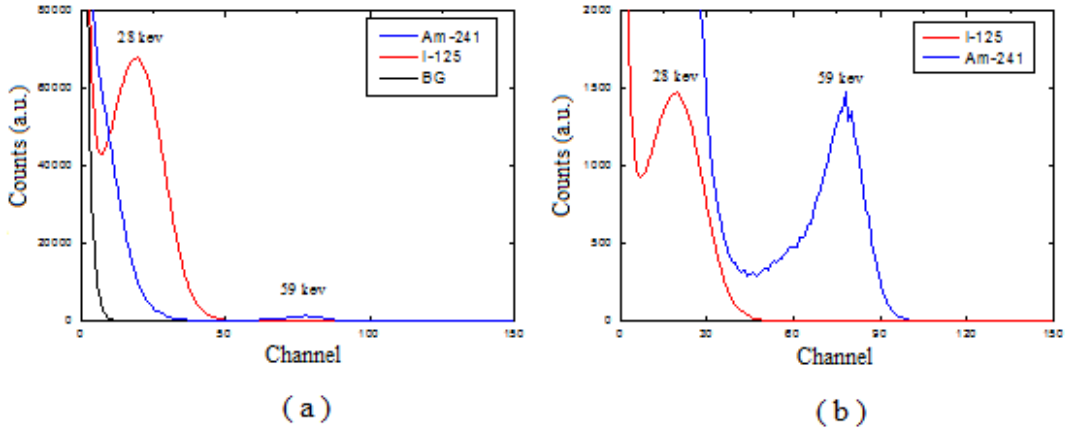

re

Figure 13: In (a), energy spectra of detector 4, when exposed to gamma radiation sources of iodine-125 and americium-241. In (b), the normalized spectra in counts. The spectra were measured with 10 MΩ bias resistance.

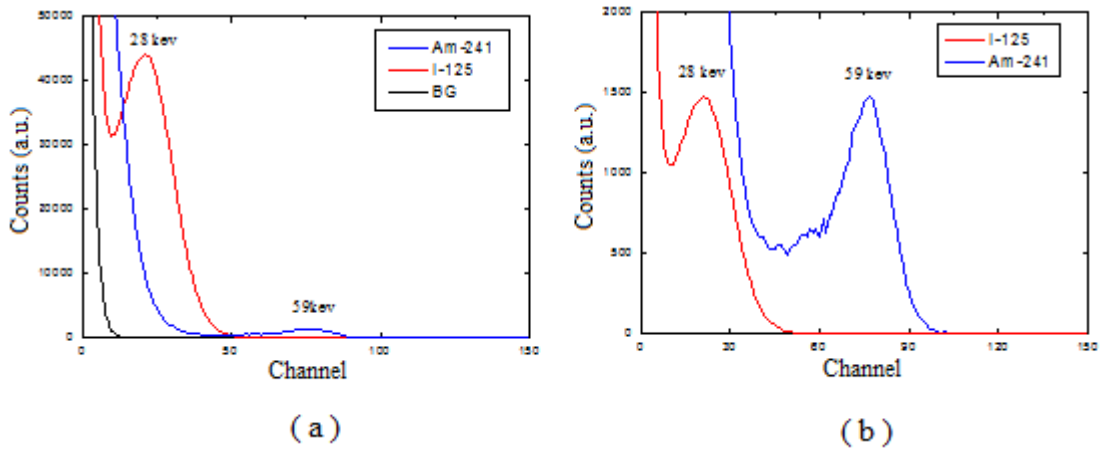

Figure 14: In (a), energy spectra of detector 4, when exposed to gamma radiation sources of iodine-125 and americium-241. In (b), the normalized spectra in counts. The spectra were measured with 250 MΩ bias resistance.

It was not possible to correlate the results of energetic resolution with the reverse current using 10 MΩ and 250 MΩ bias resistors. As for detector 3, it was clear the worse resolution at 28 keV, due to a higher reverse current related to smaller thickness, when compared with the other detectors. Better results observed for detectors 1 and 2 and the bad result for detector 3 imply that the depletion region obtained with these detectors can be closer to values between 199 and 264 µm, from the thicknesses observed for these detectors at Table 1. This behavior is in accordance with the intermediate result of detector 4 that shows an intermediate resolution between detectors 1,2 and 3; this is probably due to the high final thickness, as it can be observed in Table 1, without a higher active region. The energetic resolution obtained, which is enough to identify 28 keV and 59 keV, meets the necessity of localization of seeds, in the production process, without false positives due to noise or another close radioisotope.

CONCLUSION

The method used proved to be satisfactory for the production of surface barrier detectors with silicon substrates, for the proposed application. The passivation time should be better experimented with more substrates, to use the best thickness for the detector. The deposition time can be increased to avoid a bad deposition, as it can be occurring with detector 5.

REFERENCES

1. Stojanovic, M.; Osmakrovic P.; Boreli, F. “Characteristics of large area Silicon surface barrier detectors”, Belgrade, Institute of Nuclear Science (1997).
2. Heijne, E.H.M. ; Hubberling L. , Hyams B.D., ”A silicon surface barriers microstrip detector designed for high energy physics”, Geneve, Switzerland, CERN (1980).
3. Kim, H.S.; Park, S.H.; Ha, J.H., “Characteristics of silicon surface barrier radiation detectors for alpha particles detection”, Seoul, Hanyang University (2008).
4. Haller, E. E. , “Detector materials: Germanium and Silicon”, *IEEE Transactions on Nuclear Science*, **29**, 3, pp. 1109-1114 (1982),
5. Knoll, G. F., *Radiation Detection and Measurement*, Second Edition, John Wiley & Sons , New York, USA (1989).
6. “Amptek”, http://www.amptek.com/si_cdte.html. (2014).
7. Shiraishi, F.; Takami, Y.; Hosoe, M., “A Large Area Solid State Detector Made Ultra High Purity P-Type Si”, *Nucl. Instr. and Meth*. ,**226,** pp. 107-112 (1984)
8. Shiraishi, F.; Takami, Y.; Hosoe, M., “A Thick Surface Barrier Detectors Made of Ultra-High Purity P-Type Si Single Crystal”, *Mat. Res. Soc. Symp, Proc.*, 16, pp. 175-180 (1983).
9. Millman, J.; Halkias, C.C., *Eletrônica Dispositivos e Circuitos*, McGraw-Hill, São Paulo, Brazil (1981).